

# AIR-RELEASE AND SOLID PARTICLES SEDIMENTATION PROCESS WITHIN A HYDRAULIC RESERVOIR

*Vito Tič, Darko Lovrec*

Original scientific paper

Contaminant in a hydraulic fluid is broadly defined as any substance that impairs the proper functioning of a hydraulic system. Hydraulic fluid can be contaminated by air, particles, water, and foreign fluids. Fluid contamination can cause numerous problems including component damage, unacceptable noise, poor component response and severe fluid degradation. This paper focuses on two major contaminants that should be considered when designing a hydraulic reservoir – air and particle contamination. A proper reservoir design can prevent the occurrence of air and solid contaminants within the hydraulic system and reduce their negative effects. A hydraulic reservoir should be designed in such a way as to stabilize and direct the oil flow inside the reservoir, so that the fluid has enough time to release air bubbles and to deposit solid particles. In order to visualize and understand flow patterns inside the reservoir, all the advantages of using simulation techniques within the field of reservoir design will be shown. This paper investigates the trajectories of solid and gaseous particles within a hydraulic reservoir, which are based on simulated transient phenomena using the Ansys Workbench. The results obtained focus on the sedimentation of solid particles and the elimination of gaseous particles within a hydraulic reservoir.

**Keywords:** hydraulic reservoir, air bubbles, solid particles, simulation, trajectories

## Proces eliminacije zraka i čvrstih čestica u hidrauličkom rezervoaru

Izvorni znanstveni članak

Kontaminacija hidrauličke tekućine široko se definira kao bilo koja supstanca koja utiče na pravilno funkcioniranje hidrauličkog sistema. Hidraulička tekućina može biti kontaminirana zrakom, čvrstim česticama, vodom, i stranim tekućinama. Kontaminacija može uzrokovati brojne probleme uključujući oštećenje komponente, neprihvatljivu buku, lošu dinamiku komponenti i tešku degradaciju tekućine. Rad je usredotočen na dva glavna kontaminanta koja bi trebalo uzeti u obzir prilikom dizajniranja hidrauličkog rezervoara - kontaminacija zrakom i česticama. Ispravno dizajniran rezervoar može spriječiti pojavu zraka i čvrstih čestica u hidrauličkom sistemu i smanjiti njihove loše učinke. Rezervoar mora biti dizajniran na takav način da stabilizira i usmjerava protok ulja unutar rezervoara, tako da ima dovoljno vremena za uklanjanje mjehurića zraka i čvrstih čestica iz tekućine. Za prikaz i razumijevanje protoka uzoraka unutar rezervoara, pokazat će se prednosti korištenja simulacijskih tehnika u području dizajniranja rezervoara. U radu se istražuju putanje čvrstih i plinovitih čestica u hidrauličkom rezervoaru, bazirane na rezultatima simulacija koristeći Ansys Workbench. Dobiveni rezultati usredotočeni su na sedimentaciju čvrstih čestica i eliminaciju plinovitih čestica u hidrauličkom rezervoaru.

**Ključne riječi:** hidraulički rezervoar, zračni mjehurići, čvrste čestice, simulacija, putanje

## 1 Introduction

Besides its primary function of storing hydraulic fluid and compensating for all volume changes during a system's operation, the reservoir provides a variety of other functions that are beneficial to a system and its components. From amongst them the more important functions ensuring proper operations of all hydraulic components are air and debris separation from the oil.

A proper reservoir design for a hydraulic system is essential for the overall performance and for an individual component's life. It also becomes the principal location where the fluid can be conditioned in order to enhance its suitability. Sludge, water and foreign matter such as metal particles, have a tendency to settle down within the reservoir, whilst the captured air extracted from the oil is allowed to escape into the reservoir. This makes the construction and design of hydraulic reservoirs all the more crucial [1].

Air as a contaminant may be introduced into hydraulic fluid through improper maintenance or as a result of system design. Besides more elastic response during a system's operation, the presence of air within a hydraulic system causes oil deterioration and the degradation of lubrication, mostly pseudo cavitation, erosion, and noise generation. However, air elimination from a hydraulic fluid when the hydraulic circuit is in operation, is a difficult technical problem.

On the other hand, particle contamination accelerates the wear of hydraulic components. The rate at which

damage occurs depends on the internal clearances of the components within the system, the sizes and quantity of particles present within the fluid, and the system's pressure.

Outlined problem of captured air and air elimination in oil has been previously discussed in literature [2 ÷ 7]. Unfortunately, none of the papers describe or simulate the path of air bubbles within the hydraulic reservoir.

Some research work regarding the simulation of fluid contamination can also be found in literature [8], but unfortunately no paper could be found describing solid contaminant sedimentation within hydraulic reservoirs.

## 2 Simulation

Due to the importance of the previously outlined problem regarding captured air and particle contamination in the oil, it is necessary to know how these gaseous and solid contaminants flow through the reservoir, and whether they are eliminated. A very helpful tool for predicting the dynamical behaviour of contaminants inside a reservoir is CFD simulation based on an appropriate simulation model.

Simulations of oil-flow, containing simultaneous air bubbles and solid particles, were conducted by using the simulation tool Ansys Workbench 13.0, and were based on a real industrial 400 litre tank built according to ABMAG-NG400 standards [8] with inner dimensions of 1492 × 712 × 390 mm, as shown in Fig. 1.

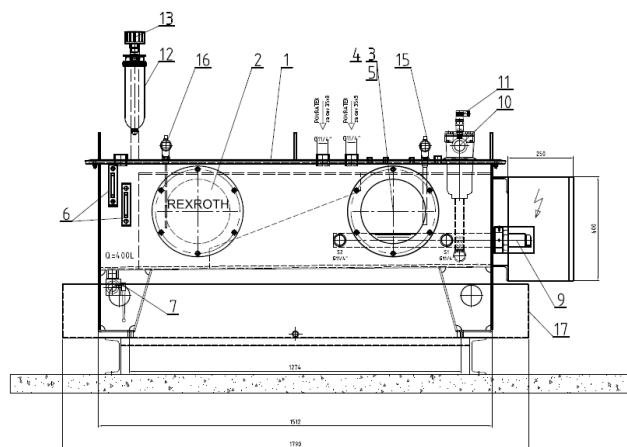


Figure 1 Simulations based on 400 L industrial tank

## 2.1 Simulation model

A model of hydraulic fluid inside the tank was developed in SolidWorks. As shown in Fig. 2 the research included three different simulation models with different inlet, outlet, and baffle positions:

- 1<sup>st</sup> model: plain vertical return line with two horizontal suction lines placed diagonally on the other side;
- 2<sup>nd</sup> model: a longitudinal baffle was placed in the middle of the reservoir. The model used the same plain vertical return line and two horizontal suction lines;
- 3<sup>rd</sup> model: vertical return line and two horizontal suction lines were placed in the same way as with the 2<sup>nd</sup> model. A diffuser was placed on the return line to help stabilize and direct the oil flow. In order to allow for proper mixing of the oil, the baffle was modified to only pass oil around the bottom area (Fig. 2).

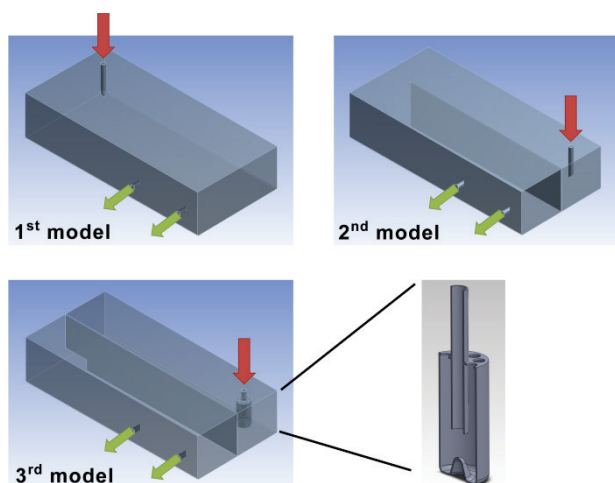


Figure 2 3D models of fluid inside the reservoir; with return tube (inlet region) and two suction tubes (outlet region)

As this is industrial practice, all return and suction pipes were cut at 45° angles.

All the inactive hydraulic pipes that existed within the actual hydraulic tank were removed to simplify the 3D model of the fluid inside the reservoir. The results of our previous research (simulation of oil-flow patterns inside the reservoir [9]) indicated that the inactive tubes do not

represent notable obstacles that would significantly change our simulation results.

During our previous work [9] it was also discovered that at given flow conditions, (described later in 2.2), the oil surface may be considered completely horizontal with no level drop from return to suction line. In order to simplify the model, the air above the oil surface was also neglected, and simulation was made with the degassing outlet condition at the top (instead of free surface-flow).

### 2.1.1 Tank mesh model

Fluid surface and volume mesh were automatically created using Ansys CFX-Mesh with regard to additional settings. The mesh was refined within the areas of the return and suction tubes, in order to obtain more realistic simulation results.

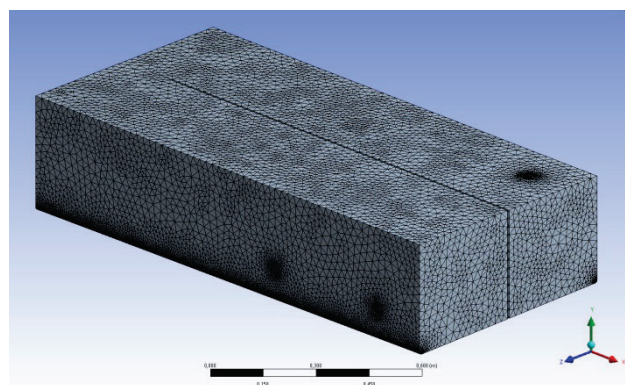


Figure 3 2<sup>nd</sup> model – generated mesh

Since the near-solid wall's boundary layers affect velocity gradients, five inflation layers were created around the tubing. The meshing results are presented in Tab. 1, and shown in Fig. 3.

Table 1 Meshing results

	Nodes	Elements
1 <sup>st</sup> Model	210,498	630,869
2 <sup>nd</sup> Model	254,029	766,012
3 <sup>rd</sup> Model	275,710	821,144

## 2.2 Simulation setup

The multiphase simulations of the research involved three homogenous materials: mineral oil (ISO VG 46), air (bubbles), and particles at constant temperature of 50 °C. The temperature influence and thus any change in fluid properties due to change in temperature, were not calculated during this simulation.

At first, a steady state simulation was performed on all models. In order to achieve better convergence of the system, the steady-state simulation was followed by transient simulations with a total time of 60 s, over time-steps of 0,1 for each.

### 2.2.1 Fluid and particle models

The mineral oil inside the fluid tank (ISO VG 46 grade) was modelled as a main continuous phase with molar-mass evaluated at about 380 kg/kmol. [10]

Since the simulation set-up neglected the temperature effects, the density of the oil was assumed to be a constant value of  $850 \text{ kg/m}^3$ . The viscosity at the given temperature was also constant and was evaluated to be  $30 \text{ cSt}$  (equivalent to ISO VG 46 viscosity at  $50 \text{ }^\circ\text{C}$ ).

One of the important parameters when simulating air-bubble and small solid particle flows in continuous viscous fluid is the surface tension coefficient. The value was found in literature and was set at  $23 \times 10^{-3} \text{ N/m}$ . [11]

Air was modelled as dispersed fluid with three different specified mean-diameters of  $20$ ,  $100$ , and  $500 \text{ }\mu\text{m}$ . In the viscous fluid, bigger air bubbles tended to rise more quickly since their lift-force (minus the viscous drag-force) was greater in comparison with the lift force of the smaller bubbles.

The most common solid particles found in the used hydraulic oil were copper particles that were also used during the simulation (copper density was approx.  $8940 \text{ kg/m}^3$  and was higher than that of steel). Similar to air bubbles, the bigger copper particles were assumed to better resist the viscous fluid-flow, and fell more quickly than the smaller ones.

## 2.2.2 Fluid interphase drag

For low Mach number flows, the drag exerted on an immersed body by a moving fluid arises from two mechanisms only. The first is due to the viscous surface shear-stress, the so-called skin friction. The second is due to the pressure distribution around the body, and is called the form-drag. The total drag force is more conveniently expressed in terms of the dimensionless drag coefficient  $C_D$ . The function may be determined experimentally, and is known as the drag-curve. ANSYS CFX offers several different models for the drag-curve, and also allows for specifying the drag coefficients directly.

Interphase drag between mineral oil and solid particles is modelled as a Schiller Naumann drag model, where the drag coefficient  $C_D$  equals [12]:

$$C_D = \frac{24}{Re} \cdot (1 + 0,15 \cdot Re^{0,687}). \quad (1)$$

CFX modifies this to ensure the correct limiting behaviour in the inertial regime by taking:

$$C_D = \max\left(\frac{24}{Re} \cdot (1 + 0,15 \cdot Re^{0,687}), 0,44\right). \quad (2)$$

During this research it was supposed that the bubbles in the dispersed phase were single-sized bubbles, whilst break-up as well as coalescence were neglected. At sufficiently small particles' Reynolds numbers (the viscous regime) the fluid particles behaved in the same manner as the solid spherical particles. Hence the drag coefficient was well-approximated by the Schiller-Naumann correlation described above. At larger particles, the Reynolds numbers, the inertial or distorted particle regimes, and the surface-tension effects became important. The fluid particles firstly became approximately ellipsoidal in shape and finally spherical cap-shaped. In this manner the Grace-drag model was

used, where the drag coefficient  $C_D$  of a single bubble equals:

$$C_D(\text{ellipse}) = \frac{4}{3} \cdot \frac{F_g \cdot d}{v_T^2} \cdot \frac{\Delta\rho}{\rho_c}, \quad (3)$$

where the terminal velocity  $v_T$  is given by:

$$v_T = \frac{\mu_c}{\rho_c \cdot d_p} \cdot M^{-0,149} \cdot (J - 0,857), \quad (4)$$

and where  $M$  is Morton's number which can be found as described in the literature, [12].

For high bubble-volume fractions, the Grace-model drag coefficient  $C_D$  may be modified using a simple power law correction:

$$C_D = r_c^p \cdot C_{D\infty}, \quad (5)$$

where  $C_{D\infty}$  is the single bubble Grace-drag coefficient and  $p$  is the volume fraction correction exponent that has negative value for small bubbles since they tend to rise more slowly at high void fractions, due to an increase in the effective mixture's viscosity.

## 2.2.3 Calculation model

The flows of the main continuous phase (mineral oil) and the dispersed phase (air) were calculated using the Eulerian-Eulerian model (together with the SST turbulence model), which is one of the two main multiphase models implemented in Ansys CFX. The other one, which is the Lagrangian Particle Tracking Model, was used to simultaneously calculate particle tracks during the main continuous phase.

## 2.2.4 Boundary conditions

There were two pumps sucking  $42 \text{ l/min}$  of oil at the suction pipes, the cross-sections of which were defined as the system's outlets. Each of the outlets was defined as having a bulk mass flow-rate of  $0,60 \text{ kg/s}$ .

The return pipe area represents the system's inlet and was defined as having the same bulk mass flow-rate as the sum of the pump flows, that is  $1,20 \text{ kg/s}$ . The flow flowing into the main domain was defined as consisting of:

- 94 % mineral oil volume fraction,
- 2 % air volume fraction with a specified bubble diameter of  $500 \text{ }\mu\text{m}$ ,
- 2 % air volume fraction with a specified bubble diameter of  $100 \text{ }\mu\text{m}$ ,
- 2 % air volume fraction with a specified bubble diameter of  $20 \text{ }\mu\text{m}$ ,
- 4 different-sized groups of copper particles with specified diameters of  $5$ ,  $25$ ,  $125$ , and  $500 \text{ }\mu\text{m}$ .

Although the particles of sizes  $125 \text{ }\mu\text{m}$  and larger are unlikely to appear in the hydraulic reservoir, they were

also simulated to show what would happen during a worst-case scenario.

In order to simulate air bubble extraction from the surface, the degassing outlet boundary condition was set at the top of the fluid domain, to enable air bubbles to escape from the domain.

### 3 Results

Different steady-state and transient simulation results were studied. Such simulation results are difficult to present on a static picture. Nevertheless, Fig. 4 shows the horizontal plane regarding the heights of suction lines (100 mm from the bottom), coloured as values of Air Volume Fraction from 0 % (blue) to 1,00 % (red). It can be clearly seen from this figure, that the 1<sup>st</sup> model presented the worst case – it extracted the least amount of air bubbles (of 500  $\mu\text{m}$ ) from the oil. The 2<sup>nd</sup> model with the plain return line and the longitudinal baffle provided a much better solution, where much less air went into the second chamber of the reservoir. The best results were obtained by the 3<sup>rd</sup> model, which used a diffuser on the return line together with a modified baffle.

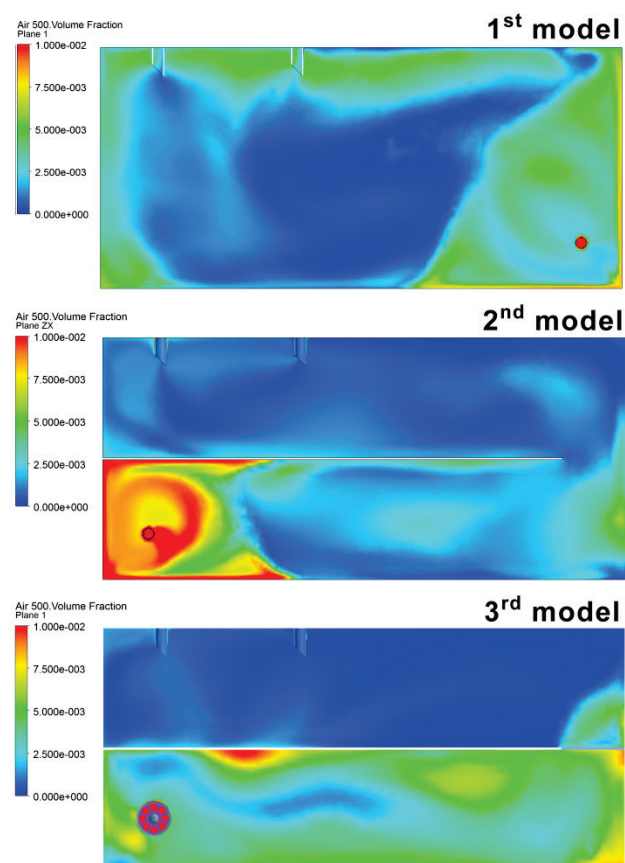


**Figure 4** Air bubbles (500  $\mu\text{m}$ ) volume fraction on a horizontal plane at a height of 100 mm, this being the suction line height

Tabs. 2 and 3 present the average air volume fractions at the outlet region, for each bubble size. In comparison to the 1<sup>st</sup> model there are approx. 4-times less air (of 500  $\mu\text{m}$  bubble size) being sucked by the pumps in the 2<sup>nd</sup> model. And further on, if we compare the 3<sup>rd</sup> and 2<sup>nd</sup> models, the pumps in the 3<sup>rd</sup> model are not even sucking half of that in the 2<sup>nd</sup> one.

**Table 2** Average air volume fraction at the outlet region

	Air bubble size		
	20 $\mu\text{m}$	100 $\mu\text{m}$	500 $\mu\text{m}$
1 <sup>st</sup> model	1,85 %	1,71 %	0,31 %
2 <sup>nd</sup> model	1,75 %	1,61 %	0,08 %
3 <sup>rd</sup> model	1,75 %	1,58 %	0,05 %

**Table 3** Percent of air extracted during flow-through

	Air bubble size		
	20 $\mu\text{m}$	100 $\mu\text{m}$	500 $\mu\text{m}$
1 <sup>st</sup> model	7,50 %	14,50 %	84,30 %
2 <sup>nd</sup> model	12,50 %	19,50 %	95,90 %
3 <sup>rd</sup> model	12,50 %	21,00 %	97,70 %

Similarly, slightly worse results were obtained by air bubbles of 100 and 20  $\mu\text{m}$  sizes. This phenomenon was due to the smaller air bubbles rising more slowly since they were experiencing less lift-force and more horizontal drag-force from the oil flow.

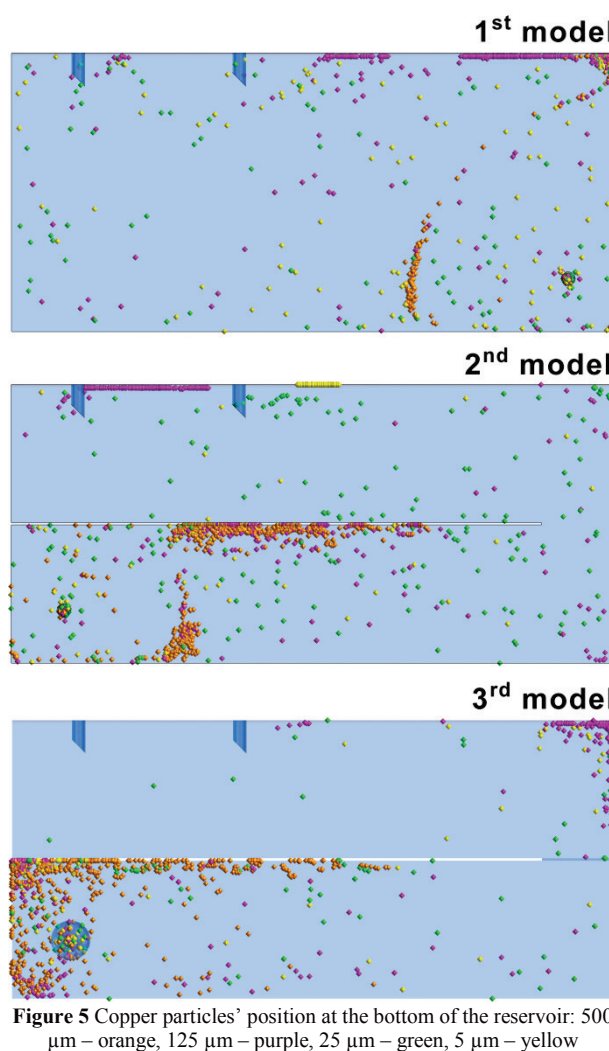


**Figure 5** Copper particles' position at the bottom of the reservoir: 500  $\mu\text{m}$  – orange, 125  $\mu\text{m}$  – purple, 25  $\mu\text{m}$  – green, 5  $\mu\text{m}$  – yellow

Fig. 5 shows the copper particles' positions regarding sizes 5, 25, 125, and 500  $\mu\text{m}$ . Again, the worst performance can be seen on the 1<sup>st</sup> model, where particles of all sizes were widely distributed inside the hydraulic tank. The exceptions were those larger particles of sizes 125 and 500  $\mu\text{m}$  (which are very unlikely to be found in a reservoir), which tended to deposit at the bottom around the return line at a certain circle. The 1<sup>st</sup> model also

displayed a dead-zone at the bottom (upper right corner in Fig. 5) where most of the particles accumulated.

The performance of the 2<sup>nd</sup> model was slightly better, since there were fewer particles found near the suction lines. It can also be seen from the figure that most of the larger particles were deposited in the first chamber.

Again, the best solution was represented by the 3<sup>rd</sup> model, which collected most of the particles within the two steady areas of oil-flow – the larger particles accumulated just near the diffuser, and the rest of the particles deposited within the first chamber or in the second chamber near the baffle (dead-zone).

### 3.1 Practical experiment

Although the simulation shows a strong improvement of flow conditions in the area around the return tube, we wanted to confirm the simulation results by an experiment on a small scaled model of the reservoir.

The model was not an exact miniature version of the presented reservoir, rather a versatile model that enabled us to monitor and observe fluid flow (and also the captured air flow) over a wide-variety of setups. The basic hydraulic plan of the unit is shown in Fig. 6 (left). An electric motor with a gear pump and frequency converter is used to allow adjustable flow through the system. On the inlet side of the pump, there is also a valve, which can be used to induce air to the system.

In order to facilitate the observations of different setups, the small scale hydraulic reservoir was made of plexus glass and equipped with a backlight.

The numerous practical experiments conducted [13] revealed very similar results and confirmed the accuracy of our simulation.

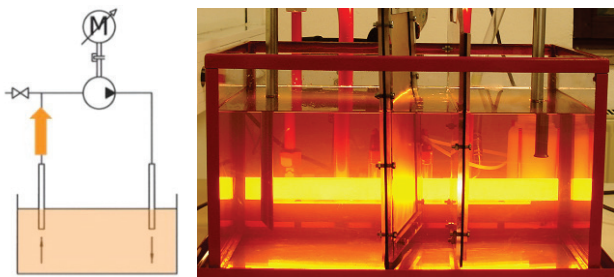


Figure 6 Small scale model used for practical experiment to confirm simulation results

### 3.2 Full- scale hydraulic reservoir

Based on the results from the simulation and the practical experiment, a full-scale hydraulic reservoir was built according to the third model. Fig. 7 presents the actual manufactured hydraulic power unit. The reservoir itself has several openings made of plexus glass, which allowed us to observe oil and air flows through the reservoir. Several of the conducted observation tests have additionally confirmed our simulation results, as well as our practical experiment results on a small scale tank.

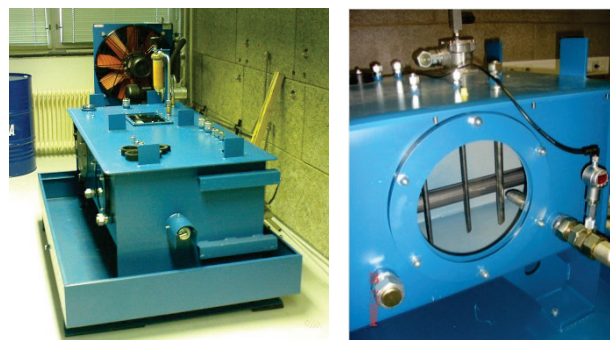


Figure 7 Hydraulic tank built according to the simulation results

## 4 Conclusion

Although this research work neglected some effects within the hydraulic reservoir (temperature, free surface flow, bubble break-up) it provided us with valuable information about what happens inside the hydraulic tank.

One of the more interesting facts revealed during the research is that those particles of sizes 5  $\mu\text{m}$  and 25  $\mu\text{m}$  (commonly found in hydraulic mineral oil) are very unlikely to be deposited during the oil-flow through the reservoir. Their mass, and thus gravitational force, is just too small to bring them to the bottom. Because the oil viscous drag-force is relatively much bigger than the gravitational force, the smaller particles tend to completely follow oil-streamlines.

Similar results were obtained by simulating the air bubble extraction. It was revealed that those smaller air bubbles of sizes 100  $\mu\text{m}$  and less are harder to extract, since they rise much more slowly in viscous fluid.

Simulation results revealed that in order to reduce the negative influence of the major contaminants (e.g. captured air and solid particles) in real hydraulic systems, designers should consider the following recommendations:

- It is reasonable to use a partition-wall or a baffle, as a simple and cheap measure to extend the oil path and give the oil more valuable time to extract the air bubbles and sediment of the solid particles.
- Partitions should be longitudinal, as they extend the oil path better and provide greater air and particle extraction.
- Partitions should be two, at most three. In a stationary tank, a larger number of partitions would be pointless.
- Using more than three partitions' results within more stationary fluid regions is undesirable.
- Use of the newly-developed diffuser greatly reduces oil swirling and significantly helps stabilize fluid flow. More stabilized fluid flow consequently results in better air and particle extraction.

### Acknowledgement



The operational part was financed by the European Union, European Social Fund. The operation was implemented within the framework of the Operational Programme for Human Resources Development for the

Period 2007 ÷ 2013, Priority axis 1: Promoting entrepreneurship and adaptability, Main type of activity 1.1.: Experts and researchers for competitive enterprises.

## 5 Symbols

$C_D$	Drag coefficient	-
$Re$	Reynolds number	-
$d$	Bubble diameter	mm
$F_g$	Gravitational force	N
$\Delta\rho$	Reynolds averaged density difference between the phases	$\text{kg/m}^3$
$\rho_c$	Reynolds averaged density of continuous phase	$\text{kg/m}^3$
$v_T$	Terminal velocity	m/s
$\mu_c$	Dynamic viscosity of continuous phase	Pa s
$r_c$	Volume fraction of continuous phase	-
$p$	Volume fraction correction exponent	-

## 6 References

- [1] Doddannavar, R.; Barnard, A. Practical Hydraulic Systems, Elsevier Science & Technology Books, 2005.
- [2] Backè, W.; Lipphardy, P. Influence of Dispersed Air on the Pressure Medium. Process Contamination of Fluid Power Systems, 1997, C97/76, pp. 77-84.
- [3] Totten, E. G.; Sun Y. H.; Bishop R. J. Hydraulic Fluids: Foaming, Air Entrainment, and Air Release – A Review, SAE Technical Paper Series, Paper Number 972789, 1997, doi:10.4271/972789.
- [4] Svedberg, G.; Totten, G.; Sun, Y.; Bishop, R. Hydraulic System Cavitation: Part II – A Review of Hardware Design – Related Effects, SAE Technical Paper 1999-01-2857, 1999, doi:10.4271/1999-01-2857.
- [5] Totten, G.; Bishop, R., The Hydraulic Pump Inlet Condition: Impact on Hydraulic Pump Cavitation Potential SAE Technical Paper 1999-01-1877, 1999, doi:10.4271/1999-01-1877.
- [6] Suzuki, R.; Tanaka, Y.; Arai, K.; Yokota, S. Bubble Elimination in Oil for Fluid Power Systems, SAE Technical Paper 982037, 1998, doi:10.4271/982037.
- [7] Xiaoying, Z.; Yunhua, L. Contamination modeling and Kalman prediction method of construction machinery hydraulic system, Fluid Power and Mechatronics (FPM), Conference publications, 2011, pp. 727-731.
- [8] N. N. Modulare Standardaggregate, Typ ABMAG, Bosch Rexroth AG, RD 51098 / 2005, p. 31.
- [9] Tič, V.; Lovrec, D. Design of modern hydraulic tank using fluid flow simulation. // International Journal of Simulation Modelling, 11, 2, 77-88, doi: 10.2507/IJSIMM11(2)2.202
- [10] Neale, M. J. Tribology Handbook, 2<sup>nd</sup> edition, Butterworth-Heinemann, 1995, Great Britain.
- [11] Totten, E. G. Handbook of Hydraulic Fluid Technology, Union Carbide Corporation, 2000, Tarrytown, New York
- [12] Ansys, Ansys 13.0 Help, 2010, Section 4.5.2. Interphase Drag for the Particle Model.
- [13] Urbančič, G. Pristop k načrtovanju hidravličnih rezervoarjev, Diploma thesis, University of Maribor, Faculty of Mechanical Engineering, 2007.

## Authors' addresses

**Vito Tič, univ. dipl. ing.**

OLMA d.d.

Poljska pot 2, SI-1000 Ljubljana, Slovenia

E-mail: vito.tic@olma.si; vito.tic@um.si

Tel.: +386 2 22 07 613

**dr. Darko Lovrec**

Univerza v Mariboru, Fakulteta za strojništvo

Smetanova 17, SI-2000 Maribor, Slovenia

E-mail: darko.lovrec@um.si

Tel.: +386 2 22 07 611